

# Accurate Analysis of JEM Interference In Airborne Array Characteristics using Parallel HO-IE-DDM

Yingyu Liu, Qin Su, Xunwang Zhao, Yu Zhang, Chang Zhai

School of Electronic Engineering

Xidian University

Xi'an, China

305296337@qq.com

**Abstract**—In this paper, we present a parallel integral equations based on domain decomposition method discretized by higher-order basis functions (HO-IE-DDM) to analyze airborne array interference problems affected by jet engine modulation. This paper proposes two main novelties. Firstly, the interfered radiation characteristics of airborne array by multiple rotating blades are analyzed using integrated simulation technology. Secondly, the recalculation amount is reduced by using HO-IE-DDM, for only re-computing the changed parts of the model during the analysis process. Numerical examples with complex electrically large structures are simulating to demonstrate the flexibility, accuracy, and efficiency of HO-IE-DDM. The compared maps show the change laws of modulation level.

**Keywords**—jet engine modulation, airborne antenna array, parallelization, higher-order MoM, domain decomposition method.

## I. INTRODUCTION

Radar is a powerful tool for detecting and tracking airborne targets. Antenna pattern as the input of radar detection performance, due to the platform nearfield scattering the antenna pattern produce distortion, the influence as the final effect on radar detection performance [1]. There are some rotating parts in an air plane like blades of turbofan engine and propeller-fan engine [1-3]. These rotating objects can cause a periodic modulation of electromagnetic (EM) wave radiated by antenna array, which is known as jet engine modulation (JEM). The effect can result in a miscalculation of radar. For a long time, researches about rotating objects are mainly limited in scattering characteristics [1-4]. For more complex EM problem, the radiation patterns of the antenna affected by JEM effect, it was not until last decade to be carried out [5]. Usually, the antennas involved are simpler structures at lower working frequency, and only one single rotor can be calculated. Due to the large electrical size of the whole targets and the complex EM environment, such electromagnetic compatibility (EMC) problem is extremely challenging. Scholars generally use high frequency algorithm like uniform geometrical theory of diffraction (UTD) [6] and physical optics (PO) to analyze JEM. However, such method fails to ensure sufficient accuracy. Using method of moment (MoM) to study JEM can get accurate results, but MoM usually generates a great computation amount [7]. It could be an effective way to solve the EM problems from electrically large structures combining the method of integral equations (IE) with DDM [8]. By

bringing parallel computing technique in the HO-IE-DDM, the simulating capability of the method is further improved.

In this paper, the radiating characteristics of a large antenna array mounted on a double rotor aircraft are analyzed using parallel HO-IE-DDM. This method provides unprecedented flexibility and convenience and is especially fit for solving the electrically large problem with changeable objects.

## II. THEORY OF HO-IE-DDM

### A. High-order MoM and Parallelization

Different from the traditional RWGs which are defined on triangle patches, the higher-order basis functions (HOBs) are defined on bilinear quadrilateral patches:

$$\mathbf{F}_{ij}(p, s) = \frac{\alpha_s}{|\alpha_p \times \alpha_s|} p^i s^j, \quad (1)$$
$$-1 \leq p \leq 1, -1 \leq s \leq 1.$$

Where  $p$  and  $s$  are the local coordinates;  $\alpha_p$  and  $\alpha_s$  are covariant unitary vectors. The surface current over a bilinear patch is decomposed into its  $p$  and  $s$  components, as shown in Fig. 1.

Introducing HOBs can produce fewer unknowns and further increase the scale of the problem to be solved. The radiation problem of an arbitrarily shaped object can be modeled with surface integral equations. The IE can be represented by a matrix equation using HOBs. The matrix equation is as follows:

$$\mathbf{Z}\mathbf{I} = \mathbf{V}. \quad (2)$$

where the coefficient matrix  $\mathbf{Z}$  is an  $N \times N$  square matrix,  $\mathbf{I}$  is the unknown current coefficient vector and  $\mathbf{V}$  is the vector of excitation.

For parallelization, the large dense MoM matrix is divided into a number of smaller block matrices that are nearly equal in size and distributed among all participating processes. The distribution manner of the blocks is chosen appropriately according to the parallel lower/upper decomposition solver to minimize the communication between processes. Parallelized HO-IE-DDM can further reduce the computational time.

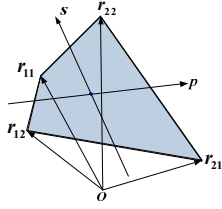


Fig. 1. Bilinear quadrilateral patch defined by four vertices with  $\mathbf{r}_{11}$ ,  $\mathbf{r}_{21}$ ,  $\mathbf{r}_{12}$  and  $\mathbf{r}_{22}$ .

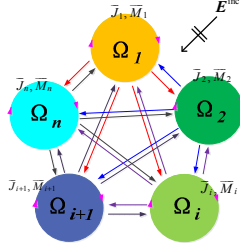


Fig. 2. Notations for domain decomposition.

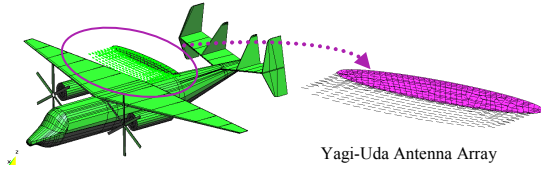


Fig. 3. Model of the double rotor aircraft mounting Yagi-Uda antenna array.

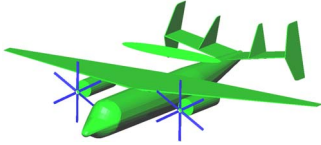


Fig. 4. Domain decomposition model (each color represents a sub-domain).

### B. Domain decomposition method

As shown in Fig. 2, the simulation model is divided into several subdomains  $\Omega_i$  ( $i=1,2,\dots,n$ ). Higher-order MoM (HOMoM) is employed for each part. The matrix (2) can be expressed as:

$$\begin{bmatrix} \mathbf{Z}_{11} & \mathbf{Z}_{12} & \cdots & \mathbf{Z}_{1n} \\ \mathbf{Z}_{21} & \mathbf{Z}_{22} & \cdots & \mathbf{Z}_{2n} \\ \vdots & \vdots & \ddots & \vdots \\ \mathbf{Z}_{n1} & \mathbf{Z}_{n2} & \cdots & \mathbf{Z}_{nn} \end{bmatrix} \begin{bmatrix} \mathbf{I}_1 \\ \mathbf{I}_2 \\ \vdots \\ \mathbf{I}_n \end{bmatrix} = \begin{bmatrix} \mathbf{V}_1 \\ \mathbf{V}_2 \\ \vdots \\ \mathbf{V}_n \end{bmatrix} \quad (3)$$

where  $\mathbf{Z}_{ij}$  ( $i=j$ ) is the self-impedance matrix in  $\Omega_i$ ,  $\mathbf{Z}_{ij}$  ( $i \neq j$ ) is the mutual impedance matrix between  $\Omega_j$  and  $\Omega_i$ ,  $\mathbf{I}_i$  is the current coefficient vector in  $\Omega_i$  and  $\mathbf{V}_i$  is the excitation vector in  $\Omega_i$ .

Noting that the mutual impedance in (3) is unnecessary to be stored, the coupling voltage ( $\Delta \mathbf{V}_i = \mathbf{Z}_{ij} \mathbf{I}_j$ ) can be obtained using the near scattered field produced by the current ( $\Delta \mathbf{V}_i(\mathbf{E}_{ij}, \mathbf{H}_{ij})$ ), and hence the memory requirement is reduced. The Jacobi method is adopted to calculate the interactions

among domains. The vector of excitation  $\mathbf{V}_i$  of  $\Omega_i$  is amended by other domains at each step.

$$\mathbf{Z}_{ii} \cdot \mathbf{I}_i = \mathbf{V}_i(\mathbf{E}^{inc}, \mathbf{H}^{inc}) + \sum_{j=1, j \neq i}^n \Delta \mathbf{V}_i(\mathbf{E}_{ij}, \mathbf{H}_{ij}). \quad (4)$$

## III. COMPUTATIONAL ANALYSIS OF JEM ON AIRBORNE ANTENNA ARRAY

HO-IE-DDM provides unprecedented flexibility and convenience for the object with changeable parts, since it just needs to re-compute the changed parts of the model during the design process, such as the analysis of antenna distribution on airborne system.

### A. Static Airborne Antenna Array Characteristics

The aircraft is  $22.03\text{m} \times 17.16\text{m} \times 6.16\text{m}$  [9]. A Yagi-Uda antenna array [10] operated in 470MHz is mounted on roughly middle of the fuselage, which consists of 36 units, and each unit has 8 directors. The aircraft model is shown in Fig. 3, which illustrates the relative location of the antenna array. Both sides of the wings are respectively equipped with a rotor. Each blade is  $1.77\text{m} \times 0.15\text{m} \times 0.03\text{m}$ . The corresponding electrical size of that is about  $2.77\lambda$  long,  $0.23\lambda$  wide,  $0.05\lambda$  thick.

In order to compare with modulation level, we spread 3D radiation pattern contour plot along  $\theta$  axis and  $\phi$  axis in Fig. 5. The 2D radiation patterns obtained by the proposed HO-IE-DDM are shown in Fig. 6, and the patterns of overall solution using HOMoM are also given for comparison. Computing information of radiation characteristics of the model analyzed by parallelized HO-IE-DDM and HOMoM is shown in Table I.

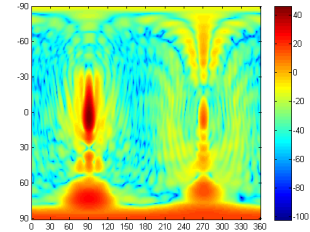


Fig. 5. Airborne array pattern.

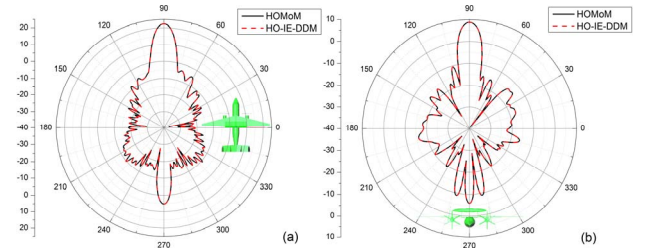


Fig. 6. 2D radiation patterns of the airborne array (a)  $\phi$  plane; (b)  $\theta$  plane.

TABLE I. COMPUTATIONAL STATISTICS OF AIRBORNE ARRAY

Method	Unknowns	Cpu cores	Storage (GB)	Time(s)
HO-IE-DDM	30324 (domain1)	12	13.70 (domain1)	1392.62
	1712 (domain2)		0.04 (domain2)	

Method	Unknowns	Cpu cores	Storage (GB)	Time(s)
HOMoM	31716	12	14.99	1424.91

a.

TABLE II. COMPUTATIONAL STATISTICS OF INTERFERED ARRAY

Method	Unknowns	Cpu cores	Storage (GB)	Time(s)
HO-IE-DDM	30324 (domain1) 1712×1024 (domain2)	12	13.70 (domain1) 0.04×1024 (domain2)	897.5×1 (domain1) 9.8s×1024 (domain2) 113542.7 (total)
HOMoM	31716×1024	12	14.99×1024	——

b.

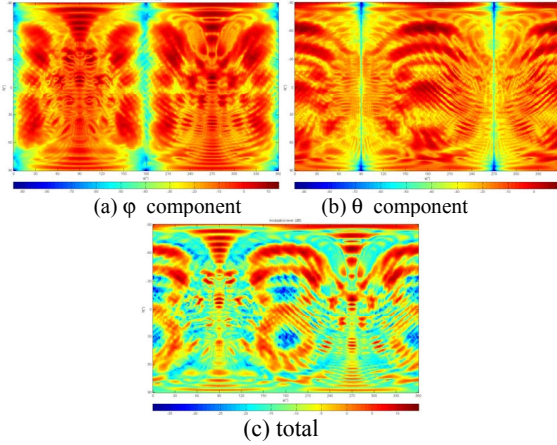


Fig. 7. Spreaded modulation level map.

#### B. Dynamic Airborne Antenna Array Characteristics on JEM

Based on quasi-stationary method, 1024 rotor orientations are included in the predictions of  $0^\circ$  to  $360^\circ$ . For each of the fixed rotor orientations, the principal plane radiation pattern is predicted. The level of rotor modulation is calculated for each observation angle. For these comparisons, the level of rotor modulation is defined as the difference between the maximum and minimum magnitudes of the electric field that occur at a given observation angle among the rotor orientations ( $\text{modulation level} = 20\lg(|E_{\max}| - |E_{\min}|)$ ). The accuracy of the proposed method has been proved in Fig. 6. Fig. 7 shows the changeable intensity of the airborne array radiation pattern at every observation angles. JEM affects less when the receiving antenna is circularly polarized. Compared with Fig. 5 there is a complementary relationship before and after the modulation. It shows that side-lobes and null depth levels of the airborne array are intensely changed.

To save computing time, the modulation level is only computed by HO-IE-DDM. Since only the small rotating part as a subdomain with the main part of the aircraft solved separately, HO-IE-DDM does not show the significant computational advantages over HOMoM in one calculation. When the rotating part rotates, it needs to perform multiple

calculations based on the position change. For HOMoM, it needs at least  $1024 \times 1424.91$ s to calculate the 1024 rotor orientations. As shown in Table II, HO-IE-DDM exhibits good performance for saving 92% of computation time compared to HOMoM.

#### IV. CONCLUSION

An efficient HO-IE-DDM algorithm is developed to solve large complex EMC problem, such as JEM airborne array interference problem. The proposed method is of great significance especially in the problems with changeable parts. The modulation level of a double rotor aircraft mounting large antenna array has been successfully obtained. Numerical results verify the feasibility and versatility of this method.

#### ACKNOWLEDGMENT

This work was supported in part by the National Key R&D Program of China under Grant 2016YFE0121600, in part by the China Postdoctoral Science Foundation funded project under Grant 2017M613068, in part by the National Key R&D Program of China under Grant 2017YFB0202102, and in part by the Special Program for Applied Research on Super Computation of the NSFC-Guangdong Joint Fund (the third phase) under Grant No.U150150.

#### REFERENCES

- [1] V. C. Chen, The micro-Doppler effect in radar, USA: Artech House, 2011.
- [2] D. Gaglione, "MACHE-model-based algorithm for classification of helicopters," IEEE A&E Systems Magazine, vol. 1, pp. 38-40, 2016.
- [3] A. K. Singh and Y. H. Kim, "Automatic measurement of blade length and rotation rate of drone using W-band micro-Doppler radar," IEEE Sensors Journal, vol. 18, pp. 1895-1902, 2018.
- [4] T. Dogaru, K. Gallagher, and C. Le, "Doppler radar phenomenology in small commercial unmanned aerial systems," U.S. Government Work, pp. 205-206, 2017.
- [5] J. E. Richie and B. R. Koch, "The use of side-mounted loop antennas on platforms to obtain nearly omnidirectional radiation," IEEE Trans. Antennas Propagat., vol. 53, pp. 3915-3919, 2005.
- [6] C. R. Birtcher, C. A. Balanis, and D. Decarlo, "Rotor-Blade Modulation on Antenna Amplitude Pattern and Polarization: Predictions and Measurements", IEEE Trans EMC, vol. 41, pp. 384-393, Nov. 1999..
- [7] Y. Zhang, T. K. Sarkar, X. Zhao, Higher order basis based integral equation solver (HOBBIES). Hoboken, New York: John Wiley, 2012.
- [8] Y. Li, X. Zhao, H. Zhang, "Out-of-Core Solver Based DDM for Solving Large Airborne Array," Applied Computational Electromagnetics Society, vol. 31, pp. 509-519, 2016.
- [9] SP Ltd, "NATOPS flight manual: Navy model E-2C plus aircraft". US Navy: Navair 01-E2AAB-1, 1999.
- [10] V. Pan'ko, Y. Salomatov, and V. Ovechkin, "Software for designing of dipole antenna arrays, multiFrequency matching with wide band antennas," Proceedings of the IEEE-Russia Conference, vol. 4, pp. 36-38, 1999.